Text S1. Sample NAMD colvars (.in) file for CheY.

```
colvar {
        name asp57od1_to_mg             # distance of carbonyl to mg
        width 0.1
        lowerboundary 1.9
        upperboundary 2.2
        lowerWallConstant 100.0
        upperWallConstant 100.0

        distance {
                group1 { atomNumbers 1986 }
                group2 { atomNumbers 875 }
        }
}

colvar {
        name asp57phos_coord_to_mg      # coordination of phosphoryl to mg

        lowerboundary 0.0
        upperboundary 1.0
        lowerWallConstant 100.0
        upperWallConstant 100.0

        coordNum {
                group1 { atomNumbers 878 879 880 }
                group2 { atomNumbers 1986}
        cutoff 3.3
        }
}

colvar {
        name mgcom                      # anchor mg to its own starting coordinates
        width 0.001

        lowerboundary 0.0
        upperboundary 0.1
        lowerWallConstant 100.0
        upperWallConstant 100.0

        distance {
                group1 { atomNumbers 1986 }
                group2 { dummyAtom (0.069, 44.943, 123.420) }
        }
}

colvar {
        name ala88n_to_asp57ot          # distance of alanine to phosphoryl to overcome initial clashes
        width 0.001

        lowerboundary 2.0
        upperboundary 3.3
        lowerWallConstant 100.0
        upperWallConstant 100.0

        distance {
```

```
                group1 { atomNumbers 1345 }
                group2 { atomNumbers 879 }
        }
}

colvar {
        name asp13_coord_to_mg          # coordination of active site aspartate to mg to allow water

        lowerboundary 0.0
        upperboundary 1.0
        lowerWallConstant 100.0
        upperWallConstant 100.0

        coordNum {
                group1 { atomNumbers 193 194 195 }
                group2 { atomNumbers 1986}
        cutoff 3.3
        }
}

colvar {
        name asp57o1p_to_mg             # distance of phosphoryl to mg
        width 0.05

        lowerboundary 2.2
        upperboundary 2.3
        lowerWallConstant 100.0
        upperWallConstant 100.0

        distance {
                group1 { atomNumbers 1986 }
                group2 { atomNumbers 878 }
        }
}

colvar {
        name asp13od1_to_mg             # distance of active site aspartate to mg

        lowerboundary 0.0
        upperboundary 2.2
        lowerWallConstant 100.0
        upperWallConstant 100.0

        distance {
                group1 { atomNumbers 194 }
                group2 { atomNumbers 1986 }
        }
}

colvar {
        name gln59co_to_mg              # distance of main chain carbonyl on D+2 to mg

        lowerboundary 0.0
        upperboundary 2.2
        lowerWallConstant 100.0
        upperWallConstant 100.0
```

```
        distance {
                group1 { atomNumbers 920 }
                group2 { atomNumbers 1986 }
        }
}
```

Table S1: Results for identification of most representative structure for CheY.
(Each medoid is the best representative model extracted from its corresponding conformer cluster)

Assigned medoid / cluster number	[1]Pop. of original cluster	% of total combined ensemble	[2]Max RMSD (Å)	T87	Y109 χ1 (degrees)	[3]W58-T87 (Å)	[4]W58-M85 (Å)	W58 χ2 (degrees)	M85 χ1 (degrees)	[5]E89-W58 (Å)	Active Site	[6]PO_3^2 geometry (degrees)
Apo	**N/A**	**N/A**	N/A	No	-25	4.2	4.3	78	70	9.1	No	N/A
BeF_3^-	**N/A**	**N/A**	**~5**	**Yes**	**76**	**3.4**	**6.6**	**136**	**-178**	**4.8**	**Yes**	**-168**
1	1575	7.5%	**~5**	**Yes**	**79**	**3.3**	5.8	79	136	5.3	No	**-167**
2	1139	5.4%	~3	**Yes**	60	**3.4**	6.1	90	**174**	5.5	No	-158
3	**6468**	**30.7%**	**~4**	**Yes**	**78**	3.5	6.3	95	-165	6.9	No	-157
4	**3019**	**14.3%**	**~5**	**Yes**	**68**	**3.3**	**6.9**	**109**	**174**	**4.9**	**Yes**	**-174**
5	**5494**	**26.1%**	**~4**	**Yes**	65	3.7	**6.5**	**104**	**176**	5.7	No	-144
6	**3187**	**15.1%**	**~4**	**Yes**	**78**	**3.2**	**7.0**	90	**-171**	**4.5**	No	-161
7	182	0.9%	**~4.5**	**Yes**	65	3.5	5.9	93	-162	5.7	No	-152

[1] conformer cluster population; [2] in the β4-α4-β5 region; [3] Cβ-Oε; [4] Cβ-Cβ; [5] Cβ-Cβ; [6] dihedral angle, phosphoanhydride bond

Summary:

Cells are shaded grey when they meet a specific criteria.

Each medoid and its corresponding cluster was assigned an arbitrary numeric designation.

Medoids from clusters 1, 2 and 7 were placed at a lower priority due to their low conformer cluster populations (Pop.)

Phosphorylation is known to induce significant changes in the β4-α4-β5 region. Structural alignment reveals changes of up to 5 Å within the area in the crystal structures. All medoids exhibited similar changes, except the medoid from cluster 2, which was placed at a lower priority.

Upon phosphorylation, T87 is known to shift to within 2.5 Å of the phosphoryl group, forming a hydrogen bond. Medoids found with this shift were assigned "Yes" in this column. T87 was found switched in 100% of the ensemble, meaning all medoids were retained. Upon phosphorylation, Y109 rotamerizes inwards, quantified by its χ1 torsion angle changing from -25° (apo) to 76° (BeF_3^-). This corresponds to a fully buried orientation. Medoids from clusters 2, 5 and 7 showed lower degrees of rotamerization and were placed at a lower priority, meaning only ~68% of the ensemble showed completely rotamerized orientations.

Phosphorylation consistently causes W58 to shift closer to T87, going from 4.2 Å to 3.4 Å (Cβ-Oε atoms). This is shown in all medoids, though medoids from clusters 3, 5 and 7 exhibited smaller shifts and were placed at a lower priority. Simultaneously, W58 shifts away from M85 upon phosphorylation. This is seen in all medoids, though medoids from clusters 1, 2, 3 and 7 showed much smaller shifts and were placed at a lower priority. W58 is known to rotamerize upon phosphorylation, measured by the χ2 side chain torsion angle (78° to 136°). This was found to a significant degree in only medoids from clusters 4 and 5, which contain ~40% of the total ensemble. M85 also rotamerizes upon phosphorylation, going from a χ1 torsion angle of 70° to -178°. Rotamerization was observed in all

medoids, though medoids from clusters 1, 3 and 7 exhibited smaller shifts and were placed at a lower priority. E89 is also known to shift down upon phosphorylation, increasing its contact with W58. This shift was found in all medoids, though strong interactions were only observed in medoids from clusters 4 and 6, which contain ~29% of the total ensemble.

Analysis of the active site geometry in each medoid revealed that all candidates displayed distorted phosphoryl group geometry (quantified by the dihedral angle of the phosphoanhydride bond) and/or K109 arrangement, except the medoid from cluster 4, which contains only ~14% of the total ensemble.

Comparing each row, the medoid from cluster 4 (red) shows the greatest number of shaded cells and was chosen as the most representative structure for phosphorylated CheY (cluster 4 contains only ~14% of the total ensemble.

Table S2: Results for identification of most representative structure for PhoP-rec.
(Each medoid is the best representative model extracted from its corresponding conformer cluster)

Assigned medoid / cluster number	[1]Pop. of original cluster	% of total combined ensemble	[2]Max RMSD (Å)	T79	Y98 χ1 (degrees)	[3]L52-T79 (Å)	[4]L52-V77 (Å)	L52 χ2 (degrees)	V77 χ1 (degrees)	[5]R81-L52 (Å)	Active Site	[6]PO_3^{2-} geometry (degrees)
Apo	**N/A**	**N/A**	N/A	No	-59	4.7	6.3	N/A	N/A	7.4	No	N/A
BeF_3^-	**N/A**	**N/A**	**~3.5**	**Yes**	**71**	**3.7**	**6.3**	**N/A**	**N/A**	**5.3**	**Yes**	**-165**
1	**4979**	**23.6%**	**~4**	No*	-59	**3.8**	**6.8**	**N/A**	**N/A**	**6.1**	No	-155
2	**2303**	**10.9%**	**~3.5**	No*	-63	**3.8**	**6.8**	**N/A**	**N/A**	**5.4**	No	**-163**
3	**6998**	**33.2%**	**~3.5**	**Yes**	-72	**3.7**	**6.4**	**N/A**	**N/A**	**6.0**	**Yes**	**-161**
4	**1961**	**9.3%**	**~3.5**	**Yes**	-62	**3.9**	**6.9**	**N/A**	**N/A**	**5.6**	**Yes**	-155
5	**4823**	**22.9%**	**~3.5**	No*	-76	**4.0**	**6.8**	**N/A**	**N/A**	**6.0**	No	-154

[1] conformer cluster population; [2] in the β4-α4-β5 region; [3] Cβ-Oε; [4] Cβ-Cβ; [5] Cβ-Cβ; [6] dihedral angle, phosphoanhydride bond
*Refers to distance between A80 amine and phosphoryl group, similar to T79

Summary:

Cells are shaded grey when they meet a specific criteria.

Each medoid and its corresponding cluster was assigned an arbitrary numeric designation.

All medoids were retained based on conformer cluster population (Pop.)

Phosphorylation is known to induce significant changes in the β4-α4-β5 region. Structural alignment reveals unusually small changes of up to 3.5 Å within the area in the crystal structures. All medoids exhibited similar levels of change and were retained.

Upon phosphorylation, T79 is known to shift to within 2.8 Å of the phosphoryl group, forming a hydrogen bond. Medoids found with this shift were assigned "Yes" in this column. This was observed in all medoids. However, the closely related A80 was found to be positioned farther away than normal in medoids from clusters 1, 2 and 5 (3.1-3.4 Å). These were placed at lower priority. Upon phosphorylation, Y98 rotamerizes inwards, quantified by its χ1 torsion angle changing from -59° (apo) to 71° (BeF_3^-). This corresponds to a fully buried orientation. No medoids were found in a fully buried orientation. A possible reason for this is addressed in the corresponding Results subsection within the text.

Phosphorylation consistently causes L52 to shift closer to T79, going from 4.7 Å to 3.7 Å (Cβ-Oε atoms), similar to the analogous residues in CheY (W58-T87). This shift is found in all medoids, meaning 100% of the total ensemble. Normally, this would suggest that L52 should also shift away from V77 (analogous to M85 in CheY). Though this is not observed in the crystal structures (where the distance is maintained at 6.3 Å), every medoid showed a slight

increase in this distance. L52 and V77 were not examined for rotamerization. However, R81 (analogous to E89 in CheY) should shift to increase contact with L52. This is seen in the crystal structures (going from 7.4 Å to 5.3 Å upon modification) as well as in every medoid structure.

Analysis of the active site geometry in each medoid revealed that only medoids from clusters 3 and 4 formed proper catalytic geometry. Medoids from clusters 2 and 5 were unable to form a complete active site due to A80. The medoid from cluster 1 had a weaker orientation of the conserved K101 residue. The medoid from cluster 4 introduced significant distortion to the phosphoryl group geometry.

Comparing each row, the medoid from cluster 3 (red) shows the greatest number of shaded cells and was chosen as the most representative structure for phosphorylated PhoP-rec (cluster 3 contains ~33% of the total ensemble).

Table S3: Results for identification of most representative structure for FixJ-rec.
(Each medoid is the best representative model extracted from its corresponding conformer cluster)

Assigned medoid / cluster number	[1]Pop. of original cluster	% of total combined ensemble	[2]Max RMSD (Å)	T82	F101 χ1 (degrees)	[3]L55-T82 (Å)	[4]L55-V80 (Å)	L55 χ2 (degrees)	V80 χ1 (degrees)	[5]H84-L55 (Å)	Active Site	[6]PO_3^{2-} geometry (degrees)
Apo	**N/A**	**N/A**	N/A	No	-41	6.6	5.3	-158	N/A	11.5	No	N/A
BeF_3^-	**N/A**	**N/A**	**~7**	**Yes**	**70**	**3.3**	**5.5**	**N/A**	**N/A**	**6.5**	**Yes**	**-177**
1	749	3.6%	~1.5	No	-58	5.8	**6.0**	**N/A**	**N/A**	11.2	No	**-138**
2	**3551**	**16.9%**	**~3.5**	**Yes**	**68**	**3.3**	5.8	**N/A**	**N/A**	**10.5**	**Yes**	-120
3	**2052**	**9.7%**	**~4.5**	No	61	**3.6**	5.4	**N/A**	**N/A**	**10.1**	No	**-153**
4	**3084**	**14.6%**	**~4**	**Yes**	62	**3.1**	**6.2**	**N/A**	**N/A**	**10.3**	**Yes**	**-140**
5	**2495**	**11.8%**	**~4**	**Yes**	**72**	**3.2**	5.9	**N/A**	**N/A**	**10.6**	No	**-130**
6	**1385**	**6.6%**	**~6.5**	**Yes**	62	3.9	**6.6**	**N/A**	**N/A**	**7.6**	**Yes**	**-131**
7	**3870**	**18.4%**	**~4.5**	**Yes**	63	**3.5**	5.8	**N/A**	**N/A**	11.0	**Yes**	-113
8	**1311**	**6.2%**	**~4**	**Yes**	**74**	**3.4**	**6.2**	**N/A**	**N/A**	**10.7**	**Yes**	**-123**
9	904	4.3%	**~3.5**	**Yes**	55	**3.3**	**6.2**	**N/A**	**N/A**	**9.5**	No	**-132**
10	**1663**	**7.9%**	**~4**	No	58	4.2	**7.4**	**N/A**	**N/A**	11.0	No	**-148**

[1] conformer cluster population; [2] in the β4-α4-β5 region; [3] Cβ-Oε; [4] Cβ-Cβ; [5] Cβ-Cβ; [6] dihedral angle, phosphoanhydride bond

Summary:

Cells are shaded grey when they meet a specific criteria.

Each medoid and its corresponding cluster was assigned an arbitrary numeric designation.

Because of the high amount of conformational variance observed for FixJ-rec, along with conflicting criteria results, the population cutoff was lowered from 1500 to 1000. Medoids from clusters 1 and 9 were placed at a lower priority due to their low conformer cluster populations (Pop.)

Phosphorylation is known to induce significant changes in the β4-α4-β5 region. Structural alignment reveals changes of up to 7 Å within the area in the crystal structures. The medoid from cluster 1 exhibited unusually small deviations in this region (< 3.5 Å) and was placed at a lower priority.

Upon phosphorylation, T82 is known to shift to within 2.7 Å of the phosphoryl group, forming a hydrogen bond. Medoids found with this shift were assigned "Yes" in this column. T82 was found switched in ~79% of the total ensemble. Medoids from clusters 1, 3 and 10 were placed at lower priority due to lack of T82 switching. Upon

phosphorylation, F101 rotamerizes inwards, quantified by its χ1 torsion angle changing from -41° (apo) to 70° (BeF_3^-). This corresponds to a fully buried orientation. Only medoids from clusters 2, 5 and 7 showed fully buried side chain orientaitons for F101 (clusters 2, 5 and 7 contain ~35% of the total ensemble).

Phosphorylation consistently causes L55 to shift closer to T82, going from 6.6 Å to 3.3 Å (Cβ-Oε atoms), similar to the analogous residues in CheY (W58-T87). This shift is found in all medoids except from cluster 1, and is weaker in medoids from clusters 6 and 10. These were placed at a lower priority. Normally, this would suggest that L55 should also shift away from V80 (analogous to M85 in CheY). A slight increase is observed in the crystal structures (5.3 to 5.5 Å), though larger changes were exhibited in every medoid. To simulate a predictive situation, medoids with little to no increases were placed at a lower priority, mimicking CheY. L55 and V80 were not examined for rotamerization. However, H84 (analogous to E89 in CheY) should shift to increase contact with L55. This is seen in the crystal structures (going from 11.5 Å to 6.5 Å upon modification). However, H84 is flanked on by glycine residues and exhibits extremely high flexibility during simulation. It is likely that this relationship is less homologous to the CheY E89-W58 shift. Every medoid showed a decrease in this distance, though only the medoid from cluster 6 showed a large change. The medoid from cluster 6 was also eliminated based on its partially exposed aromatic switch residue orientation. Because of this, any medoid exhibiting an H84-L55 distance of < 11 Å was retained.

Analysis of the active site geometry in each medoid revealed that only medoids from clusters 4, 6, 7 and 8 formed a proper catalytic geometry. The other medoids (from clusters containing ~37% of the total ensemble) do not resemble the apo conformation, but their side chain arrangement is non-optimal. Significantly more phosphoryl group geometry distortion was observed for FixJ-rec, also seen in the experimental crystal structures. However, medoids from clusters 2 and 7 exhibited reverse orientation of the phosphorylatable aspartate residue and were placed at a lower priority.

Comparing each row, the medoid from cluster 8 (red) shows the greatest number of shaded cells and was chosen as the most representative structure for phosphorylated FixJ-rec (cluster 8 contains an unusually low ~6% of the total structural ensemble).

Table S4: Results for identification of most representative structure for Sln1-rec.
(Each medoid is the best representative model extracted from its corresponding conformer cluster)

Assigned medoid / cluster number	[1]Pop. of original cluster	% of total combined ensemble	[2]Max RMSD (Å)	T1173	F1192 χ1 (degrees)	[3]V1145-T1173 (Å)	[4]V1145-A1171 (Å)	V1145 χ2 (degrees)	A1171 χ1 (degrees)	[5]F1175-V1145 (Å)	Active Site	[6]PO_3^{2-} geometry (degrees)
Apo	**N/A**	**N/A**	N/A	No	-41	4.4	5.2	N/A	N/A	7.5	No	N/A
BeF_3^-	**N/A**	**N/A**	**~3**	**Yes**	**63**	**3.9**	**6.4**	**N/A**	**N/A**	**5.8**	**Yes**	**-174**
1	**6307**	**29.9%**	**~3**	**Yes**	47	**3.8**	5.4	**N/A**	**N/A**	6.6	No	**-151**
2	**5482**	**26.0%**	~2.5	**Yes**	53	**3.9**	5.9	**N/A**	**N/A**	6.3	**Yes**	**-153**
3	**5246**	**24.9%**	**~3**	**Yes**	**64**	**3.9**	**6.4**	**N/A**	**N/A**	8.6	**Yes**	**-152**
4	**2533**	**12.0%**	**~3**	**Yes**	**60**	**3.7**	**6.3**	**N/A**	**N/A**	6.6	No	**-174**
5	1496	7.1%	**~4**	**Yes**	38	**3.8**	5.9	**N/A**	**N/A**	6.7	No	**-161**

[1] conformer cluster population; [2] in the β4-α4-β5 region; [3] Cβ-Oε; [4] Cβ-Cβ; [5] Cβ-Cβ; [6] dihedral angle, phosphoanhydride bond

Summary:

Cells are shaded grey when they meet a specific criteria.

Each medoid and its corresponding cluster was assigned an arbitrary numeric designation.

The medoid from cluster 5 was placed at a lower priority due to its smaller cluster population (Pop.)

Phosphorylation is known to induce significant changes in the β4-α4-β5 region. Structural alignment reveals unusually small changes of up to ~3 Å within the area in the crystal structures. All medoids exhibited similar levels of change and were retained, except the medoid from cluster 2.

Upon phosphorylation, T1173 is known to shift to within 2.6 Å of the phosphoryl group, forming a hydrogen bond. Medoids found with this shift were assigned "Yes" in this column. This was observed in all medoids. Upon phosphorylation, F1192 rotamerizes inwards, quantified by its χ1 torsion angle changing from -41° (apo) to 63° (BeF_3^-). This corresponds to a fully buried orientation. Medoids from clusters 3 and 4 also exhibited this fully buried orientation. Medoids from clusters 1, 2 and 5 showed only partial rotamerization.

Phosphorylation consistently causes V1145 to shift closer to T1173, going from 4.4 Å to 3.9 Å (Cβ-Oε atoms), similar to the analogous residues in CheY (W58-T87). This shift is found in all medoids, meaning 100% of the ensemble. This suggests that V1145 should also shift away from A1171 (analogous to M85 in CheY). This is seen in the crystal structures, going from 5.2 Å to 6.4 Å. An increase is observed in every medoid, though medoids from clusters 1, 2 and 5 showed much smaller shifts and were placed at a lower priority. V1145 and A1171 were not examined for rotamerization. F1175 (analogous to E89 in CheY) was expected to shift towards V1145, as seen in the crystal structures. Minor shifts were seen in all medoids except the medoid from cluster 3. However, since the medoid from cluster 3 was the only candidate that met the other criteria, it was retained.

Analysis of the active site geometry in each medoid revealed that only medoids from clusters 2 and 3 formed a proper catalytic geometry. In medoids from clusters 1, 4 and 5, residues E1094 and D1095 were unable to coordinate the divalent Mg^{2+}.

Comparing each row, the medoid from cluster 3 (red) shows the greatest number of shaded cells and was chosen as the most representative structure for phosphorylated Sln1-rec (cluster 3 contains ~25% of the total ensemble.

Table S5. Results for identification of most representative structure for Spo0F.
(Each medoid is the best representative model extracted from its corresponding conformer cluster)

Assigned medoid / cluster number	[1]Pop. of original cluster	% of total combined ensemble	[2]Max RMSD (Å)	T82	H101 χ1 (degrees)	[3]M55-T82 (Å)	[4]M55-I80 (Å)	M55 χ2 (degrees)	I80 χ1 (degrees)	[5]E89-M55 (Å)	Active Site	[6]PO_3^{2-} geometry (degrees)
Apo	N/A	N/A	N/A	No	-39	4.5	5.6	-54	-67	7.3	No	N/A
BeF_3^-	**N/A**	**N/A**	**~3.5**	**Yes**	**-61**	**3.2**	**6.0**	**-49**	**169**	**5.8**	**Yes**	**-143**
1	1180	5.6%	~2.5	No	**-48**	4.2	6.0	**-71**	-73	7.8	No	**178**
2	**1831**	**8.7%**	**~3.5**	**Yes**	**-65**	**3.8**	**7.0**	**-81**	**191**	**6.7**	**Yes**	**-160**
3	1434	6.8%	~2.5	**Yes**	53	4.0	6.8	**-67**	**195**	**6.7**	**Yes**	-159
4	**1740**	**8.3%**	**~3.5**	**Yes**	43	4.1	**7.1**	**-77**	-84	7.0	**Yes**	-158
5	**4567**	**21.7%**	**~4**	**Yes**	43	**3.8**	6.7	**-59**	-79	8.1	**Yes**	**-179**
6	**3228**	**15.3%**	**~4**	**Yes**	33	4.1	6.6	**-79**	-67	**6.4**	No	**-175**
7	1135	5.4%	**~9**	**Yes**	38	4.2	6.3	-176	**182**	9.0	**Yes**	**-173**
8	**2009**	**9.5%**	~3	**Yes**	42	**3.7**	6.9	**-71**	-81	8.0	**Yes**	**-166**
9	**2000**	**9.5%**	**~4**	**Yes**	49	4.0	**7.3**	**-80**	-77	7.0	**Yes**	**-170**
10	1053	5.0%	~2.5	**Yes**	51	3.9	6.7	**-56**	**192**	**6.2**	**Yes**	**173**
11	511	2.4%	**~5**	**Yes**	55	**3.7**	**7.1**	**-73**	-71	**6.4**	**Yes**	**179**
12	376	1.8%	**~4**	**Yes**	59	4.2	6.4	**-67**	-67	7.5	**Yes**	**-179**

[1] conformer cluster population; [2] in the β4-α4-β5 region; [3] Cβ-Oε; [4] Cβ-Cβ; [5] Cβ-Cβ; [6] dihedral angle, phosphoanhydride bond

Summary:

Cells are shaded grey when they meet a specific criteria.

Each medoid and its corresponding cluster was assigned an arbitrary numeric designation.

Medoids from clusters 1, 3, 7, 10, 11 and 12 were placed at a lower priority due to their smaller cluster populations (Pop.)

Phosphorylation is known to induce significant changes in the β4-α4-β5 region. Structural alignment reveals changes of up to ~4 Å within the area in the crystal structures. Medoids from clusters 4, 5, 6, 7, 9, 11 and 12 exhibited changes from 4-9 Å and were retained. Medoids from clusters 1, 3, 8 and 10 were placed at a lower priority because of their smaller deviations.

Upon phosphorylation, T82 is known to shift to within 2.6 Å of the phosphoryl group, forming a hydrogen bond. Medoids found with this shift were assigned "Yes" in this column. This was observed in all candidates except the medoid from cluster 1. Upon phosphorylation, H101 was found to remain fully solvent exposed, closely resembling the apo orientation (-39° and -61°). This was found only in medoids from clusters 1 and 2. Medoids from clusters 3-12 exhibited partial rotamerization, adopting intermediate orientations (clusters 3-12 contain ~86% of the total ensemble). These medoids were placed at a lower priority.

Phosphorylation consistently causes M55 to shift closer to T82, going from 4.5 Å to 3.2 Å (Cβ-Oε atoms), similar to the analogous residues in CheY (W58-T87). Significant shifts between these residues were only observed in medoids from clusters 2, 5, 8 and 11. This suggests that M55 should also shift away from I80 (analogous to M85 in CheY). This is seen in the crystal structures, going from 5.6 Å to 6.0 Å. An increase is observed in every medoid, though medoids with the largest changes were placed at a higher priority. M55 was also examined for rotamerization (analogous to W58 in CheY). In the crystal structures, no significant rotamerization was observed, unlike in CheY. Only the medoid from cluster 7 showed a significant rotamerization and was placed at a lower priority. I80 rotamerization was also examined. In the crystal structures, we see a change in the $\chi 1$ torsion angle from -67° (apo) to 169° (BeF_3^-). Similar significant rotamerizations are only found in medoids from clusters 2, 3, 7 and 10. E86 (likely analogous to E89 in CheY) was expected to shift towards M55. This is observed in the crystal structures, shifting from 7.3 Å (apo) to 5.8 Å (BeF_3^-). Medoids from clusters 2, 3, 6, 10 and 11 showed similar significant shifts. Medoids from clusters 1, 4, 5, 7, 8, 9 and 12 were placed at a lower priority because they lacked this change.

Analysis of the active site geometry in each medoid revealed that all formed correct active site geometry arrangements except medoids from clusters 1 and 6, which showed distortion of the K104 residue.

Comparing each row, the medoid from cluster 2 (red) shows the greatest number of shaded cells and was chosen as the most representative structure for phosphorylated Spo0F (cluster 2 contains only ~9% of the total structural ensemble).

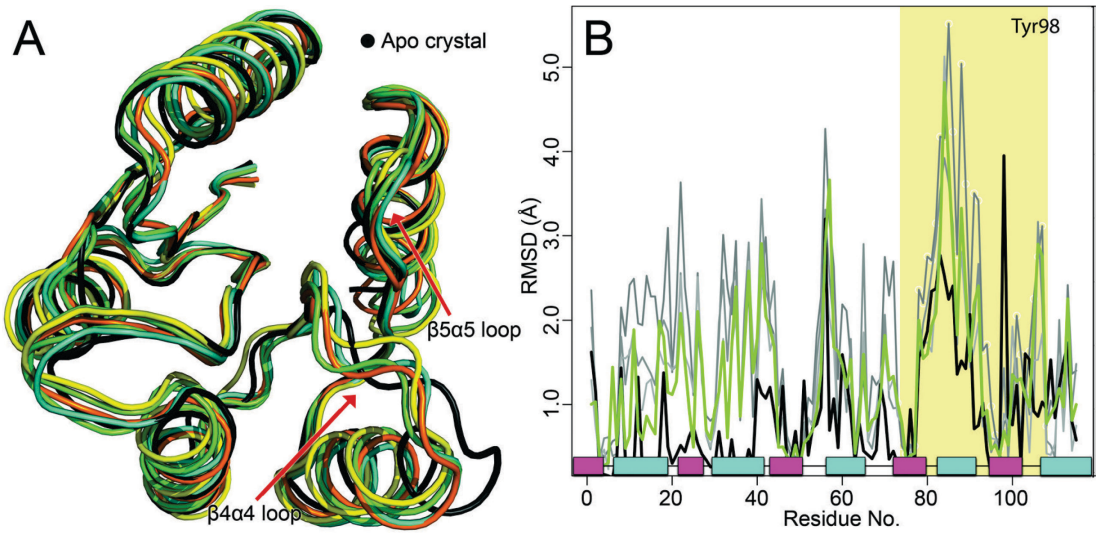

Fig. S1. Alignments of candidate structures to the unphosphorylated crystal structure of PhoP-rec. (A) Superposition of apo crystal structure (PDB 2PKX:A; black) with candidate (medoid) structures identified during cluster analysis. (B) Per residue all-atom RMSD for phosphorylated structures vs. the apo crystal structure. Shaded area corresponds to β4-α4-β5 regions. Trace color corresponds to chosen structures in alignment: example candidate structure vs. apo crystal (lime); BeF_3^- crystal vs. apo crystal (black). Traces for additional candidate structures appear in gray. α-helix (cyan); β-strand (magenta).

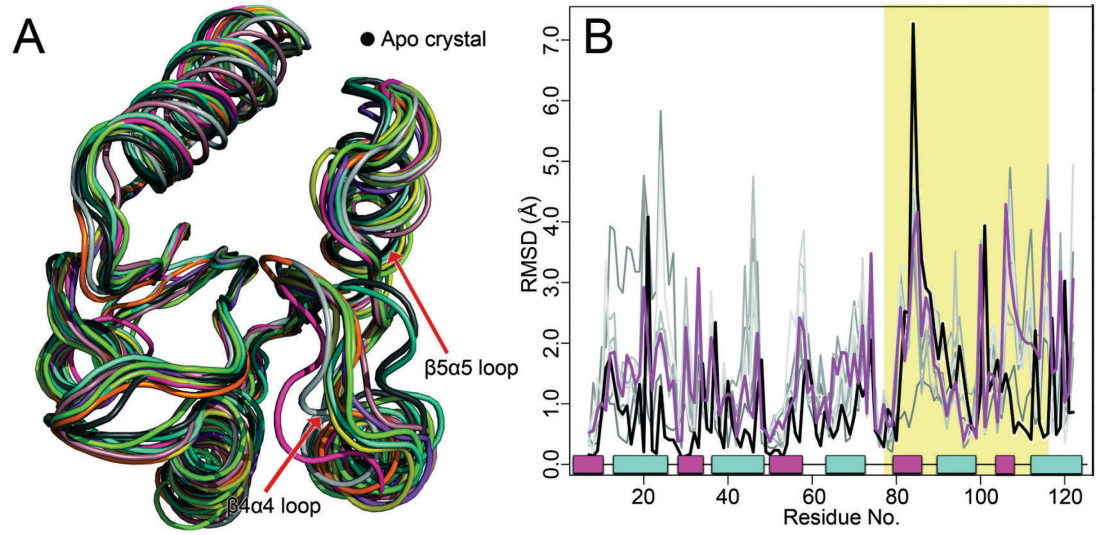

Fig. S2. **Alignments of candidate structures to the unphosphorylated crystal structure of FixJ-rec.** (A) Superposition of apo crystal structure (PDB 1DCK:A; black) with candidate (medoid) structures identified through cluster analysis. (B) Per residue all-atom RMSD for phosphorylated structures vs. the apo crystal structure. Shaded area corresponds to β4-α4-β5regions. Trace color corresponds to chosen structures in alignment: example candidate structure vs. apo crystal (purple); phosphorylated crystal vs. apo crystal (black). Traces for additional candidate structures appear in gray. α-helix (cyan); β-strand (magenta).

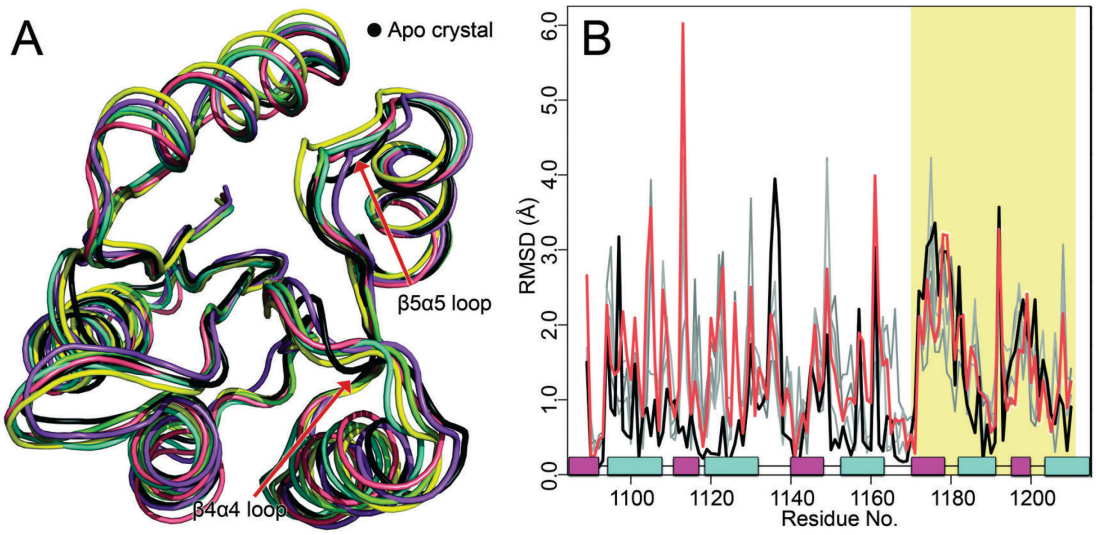

Fig. S3. Alignments of candidate structures to the unphosphorylated crystal structure of Sln1-rec. (A) Superposition of apo crystal structure (PDB 1OXB:B; black) with candidate (medoid) structures identified through cluster analysis. (B) Per residue all-atom RMSD for phosphorylated structures vs. the apo crystal structure. Shaded area corresponds to β4-α4-β5regions. Trace color corresponds to chosen structures in alignment: example candidate structure vs. apo crystal (salmon); BeF_3^- crystal vs. apo crystal (black). Traces for additional candidate structures appear in gray. α-helix (cyan); β-strand (magenta).

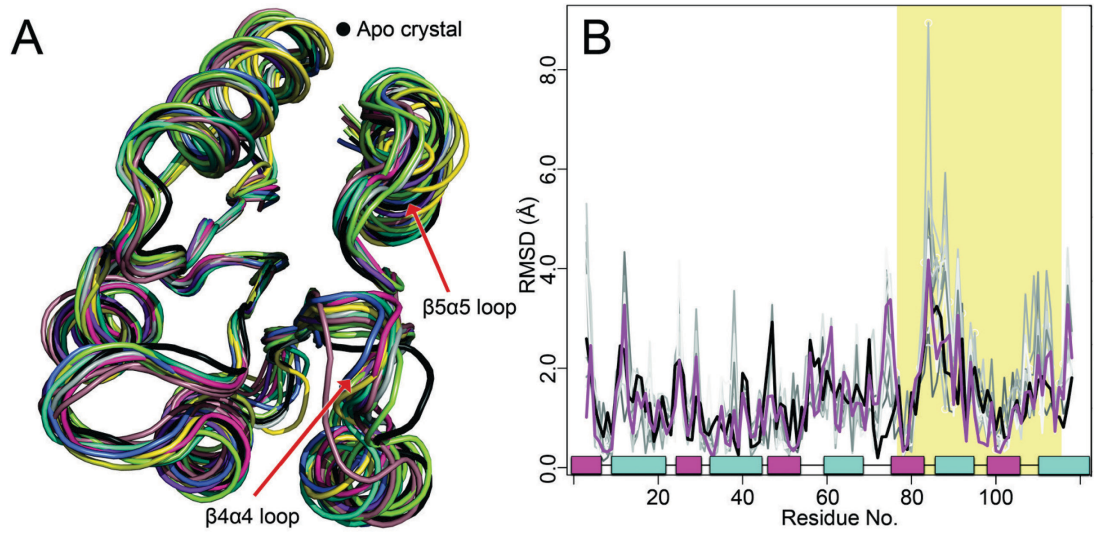

Fig. S4. Alignments of candidate structures to the unphosphorylated crystal structure of Spo0F. (A) Superposition of apo crystal structure (PDB 1NAT; black) with candidate (medoid) structures identified through cluster analysis. (B) Per residue all-atom RMSD for phosphorylated structures vs. the apo crystal structure. Shaded area corresponds to β4-α4-β5regions. Trace color corresponds to chosen structures in alignment: example candidate structure vs. apo crystal (purple); BeF_3^- crystal vs. apo crystal (black). Traces for additional candidate structures appear in gray. α-helix (cyan); β-strand (magenta).

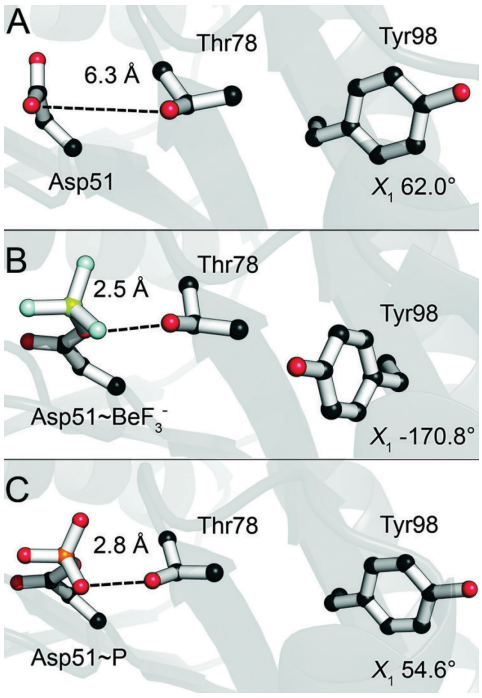

Fig. S5. Characteristic switch residues shift upon phosphorylation of PhoP-rec. (A) Apo orientation (PDB 2PKX:A). (B) Phosphorylated orientation (PDB 2PL1). Thr78 has shifted to form a hydrogen bond with Asp51. Tyr98 has rotamerized inwards into the hydrophobic pocket. (C) A sample candidate structure of phosphorylated PhoP-rec shows Thr78 orientation is identical to the BeF_3^- bound crystal. Tyr98 remains in the solvent-exposed orientation. Examination of the BeF_3^- bound structure of PhoP-rec reveals that the receiver domain crystallizes as a homodimer. Tyr98 is located in the central region of the dimerization inteface, suggesting that its side chain orientation plays an important role in dimerization and vice versa.

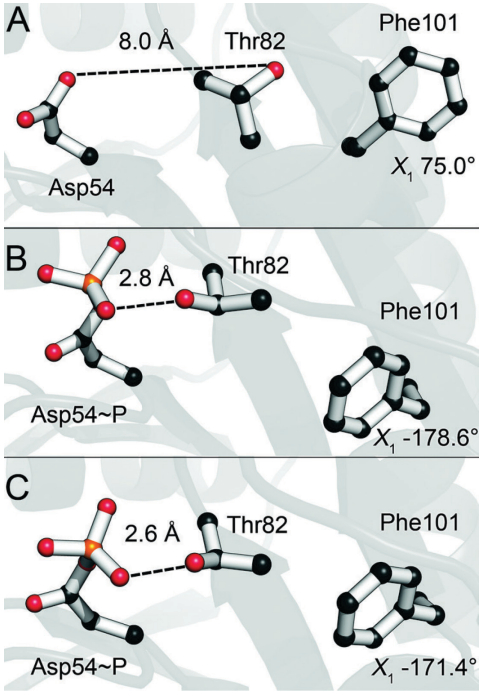

Fig. S6. Characteristic switch residues shift upon phosphorylation of FixJ-rec. (A) Apo orientation (PDB 1DCK:A). (B) Phosphorylated orientation (PDB 1D5W:A). Thr82 has shifted to form a hydrogen bond with Asp54.

Phe101 has rotamerized inwards into the hydrophobic pocket. (C) A sample candidate structure of phosphorylated FixJ-rec demonstrates near-identical orientations to the phosphorylated crystal.

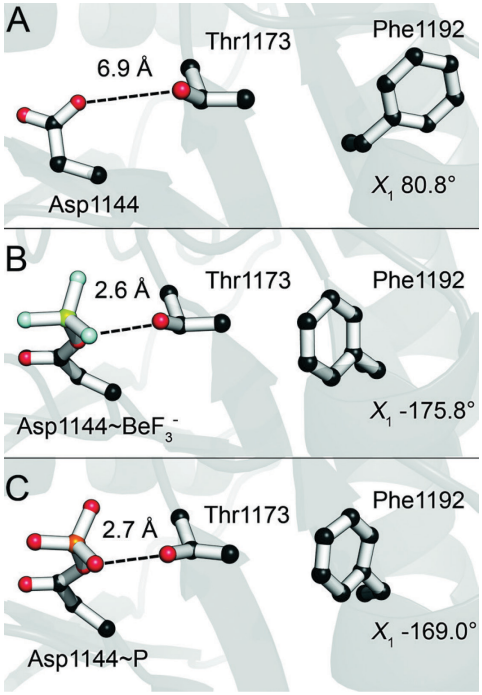

Fig. S7. Characteristic switch residues shift upon phosphorylation of Sln1-rec. (A) Apo orientation (PDB 1OXB:B). (B) Phosphorylated orientation (PDB 2R25:B). Thr1173 has shifted to form a hydrogen bond with Asp1144. Phe1192 has rotamerized inwards into the hydrophobic pocket. (C) A sample candidate structure of phosphorylated Sln1-rec demonstrates near-identical orientations to the BeF_3^- bound crystal.

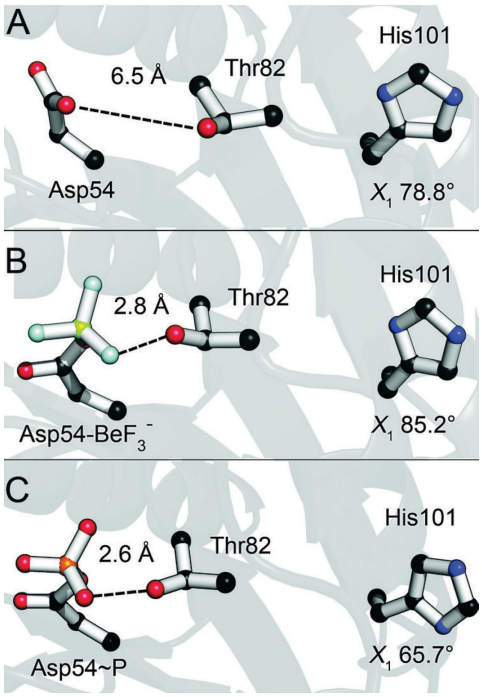

Fig. S8. Characteristic switch residues shift upon phosphorylation of Spo0F. (A) Apo orientation (PDB 1NAT:A). Thr82 is too far to form a hydrogen bond with the phosphorylatable aspartate, and His101 is solvent exposed, pointing away from the active site. (B) Phosphorylated orientation (PDB 2FTK:G). Thr82 has shifted to form a hydrogen bond with Asp54. His101 remains solvent-exposed. (C) A sample candidate structure of phosphorylated Spo0F demonstrates near-identical orientations to the BeF_3^- bound crystal. His101 remains solvent exposed.

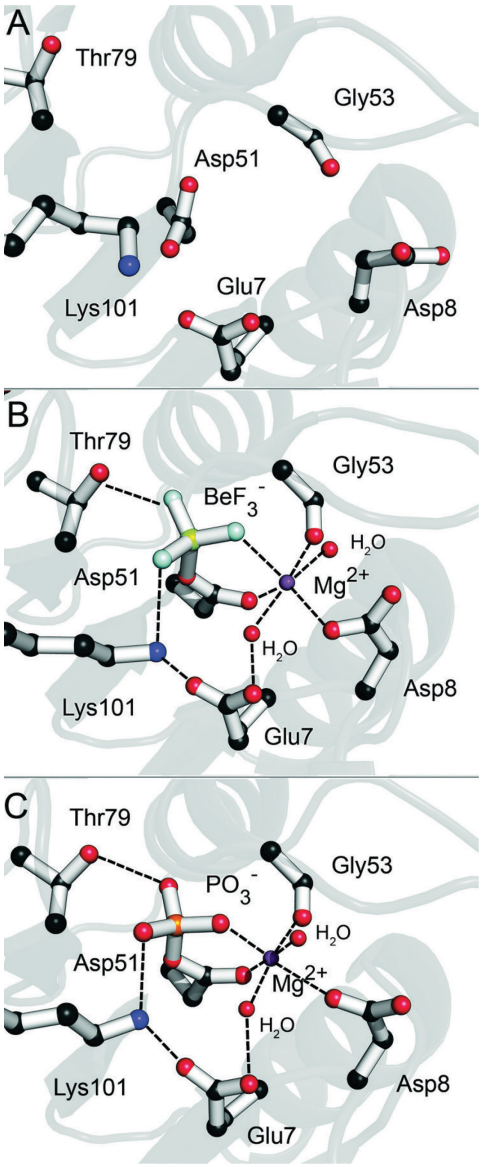

Fig. S9. Highly conserved active site geometry of PhoP-rec. (A) Disordered active site side chains of apo PhoP-rec (PDB 2PKX:A). (B) Active site side chains of PhoP-rec bound to BeF_3^- (PDB 2PL1). The addition of Mg^{2+} orders the active site, generating an octahedral coordination geometry with the recruitment of two additional water molecules. Switch residue Thr79 has shifted to hydrogen bond with Asp51. (C) Active site side chains in a sample candidate structure of phosphorylated PhoP-rec demonstrates near-identical geometry to the BeF_3^- bound crystal.

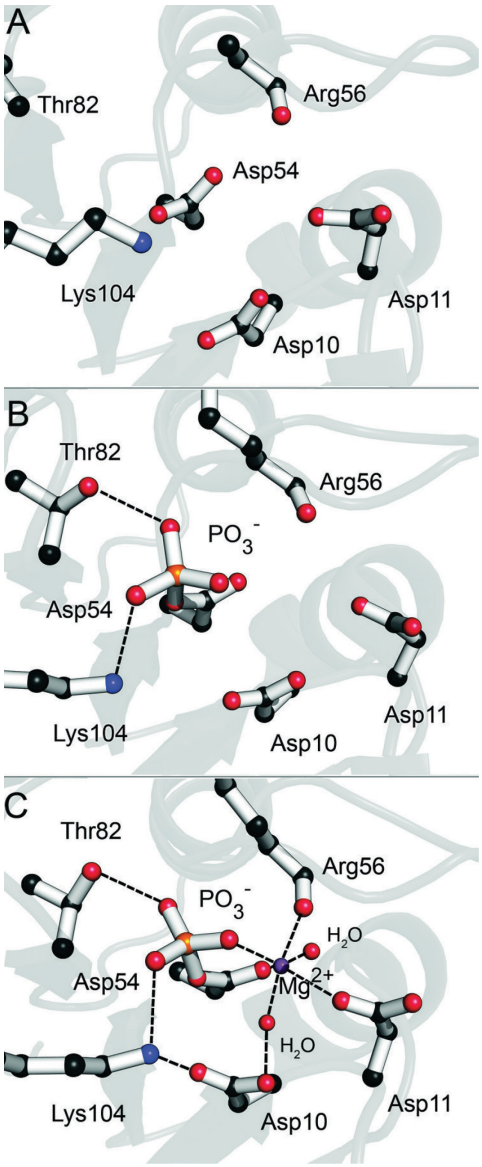

Fig. S10. Highly conserved active site geometry of FixJ-rec. (A) Disordered active site side chains of apo FixJ-rec (PDB 1DCK:A). (B) Active site side chains of phosphorylated FixJ-rec (PDB 1D5W:A). Crystal structure lacks defined waters and the metal cation. Switch residue Thr82 has shifted to hydrogen bond with Asp54. (C) Active site side chains in a sample candidate structure of phosphorylated FixJ-rec demonstrates near-identical geometry to the phosphorylated crystal.

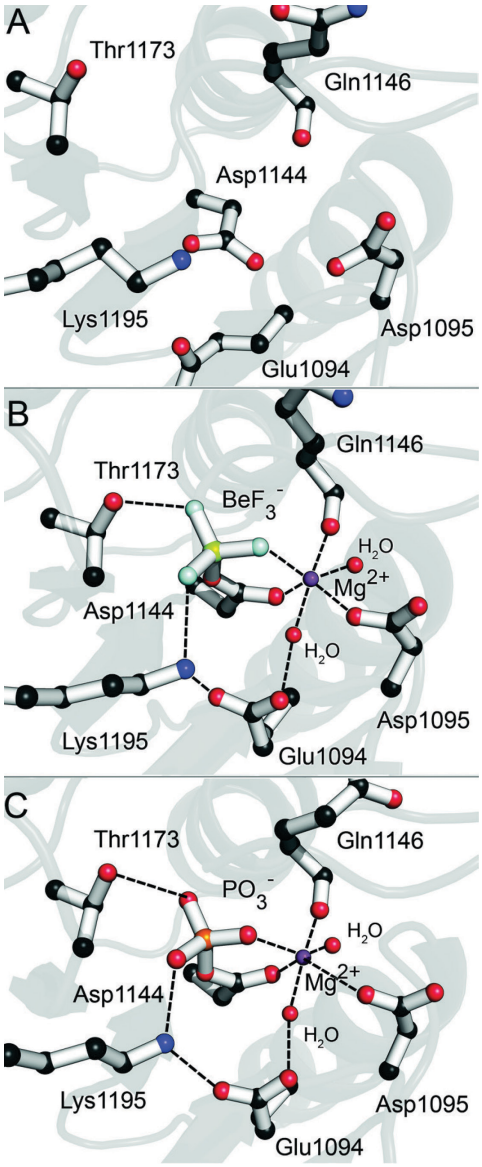

Fig. S11. Highly conserved active site geometry of Sln1-rec. (A) Disordered active site side chains of apo Sln1-rec (PDB 1OXB:B). (B) Active site side chains of Sln1-rec bound to BeF_3^- (PDB 2R25:B). The addition of Mg^{2+} orders the active site, generating an octahedral geometry with the recruitment of two additional water molecules. Switch residue Thr1173 has shifted to hydrogen bond with Asp1144. (C) Active site side chains in a sample candidate structure of phosphorylated Sln1-rec demonstrates near-identical geometry to the BeF_3^- bound crystal.

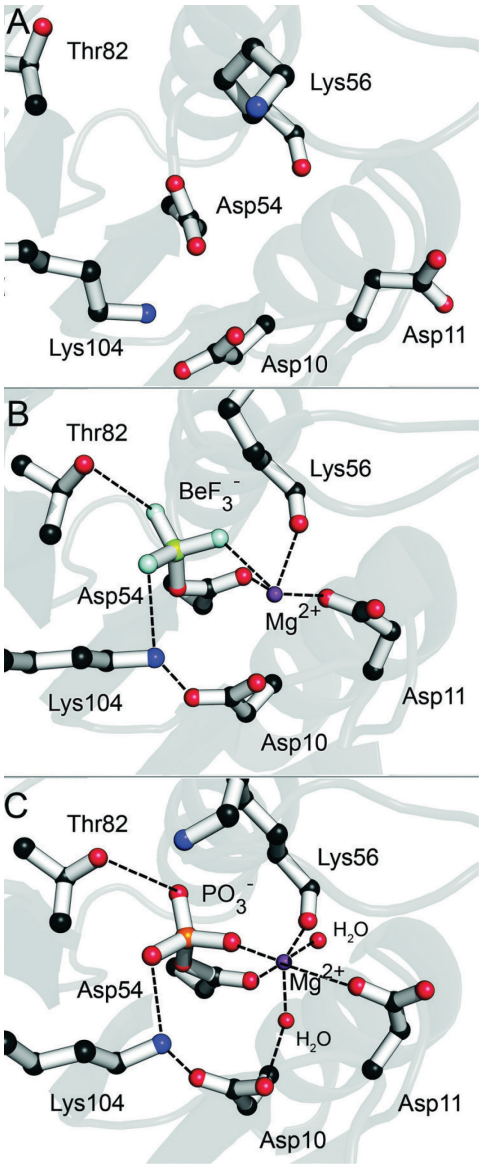

Fig. S12. Highly conserved active site geometry of Spo0F. (A) Disordered active site side chains of apo Spo0F (PDB 1NAT:A). (B) Active site side chains of Spo0F bound to BeF_3^- (PDB 2FTK:G). The addition of Mg^{2+} orders the active site, generating an octahedral geometry (note: water molecules were not defined in the crystal structure). Switch residue Thr82 has shifted to hydrogen bond with Asp54. (C) Active site side chains in a sample candidate structure of phosphorylated Spo0F demonstrates near-identical geometry to the BeF_3^- bound crystal.

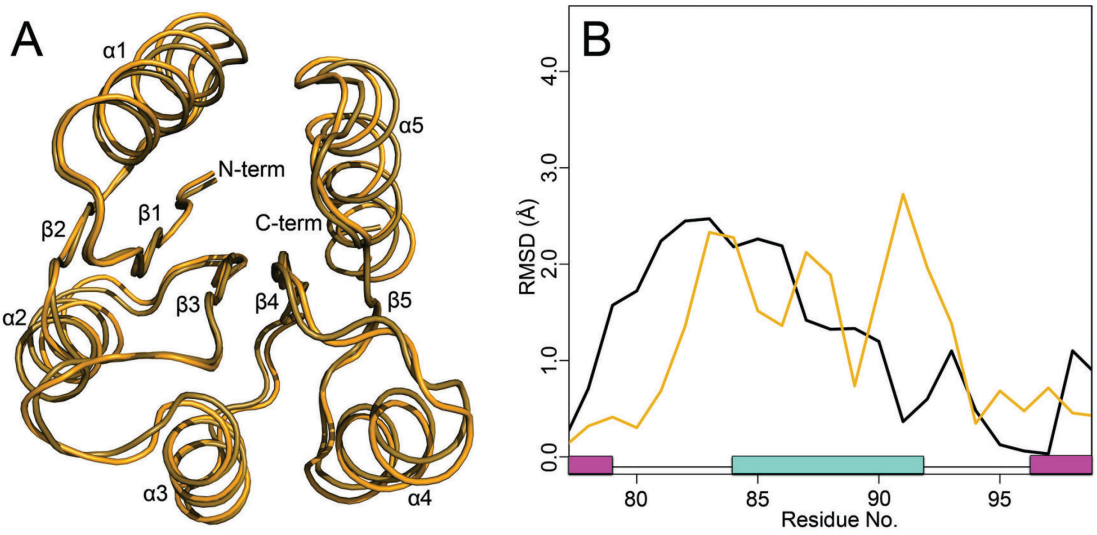

Fig. S13. Global structural alignment of the top representative model to the BeF_3^- bound crystal structure of PhoP-rec and comparisons of the β4-α4-β5 region. (A) Final predicted model (gold). Crystal structure of PhoP-rec with BeF_3^- bound (PDB 2PL1, brown). (B) Per-residue RMSD for apo vs. BeF_3^- crystals (black), and for predicted model vs. BeF_3^- crystal (gold). The black trace shows the differences between the BeF_3^- bound and apo conformation. The gold trace shows how closely the prediction matches the true experimental structure. α-helix (cyan); β-strand (magenta).

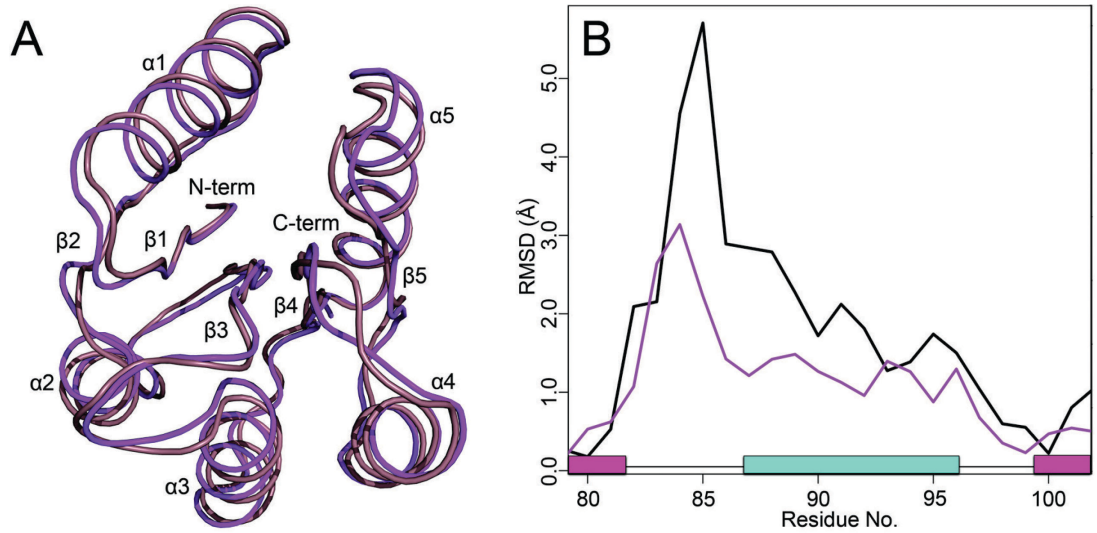

Fig. S14. Global structural alignment of the top representative model to the phosphorylated crystal structure of FixJ-rec and comparisons of the β4-α4-β5 region. (A) Final predicted model (magenta). Phosphorylated crystal structure of FixJ-rec (PDB 1D5W:A, dark purple). (B) Per-residue RMSD for apo vs. phosphorylated crystals (black), and for predicted model vs. phosphorylated crystal (magenta). The black trace shows the differences between the phosphorylated and apo conformation. The magenta trace shows how closely the prediction matches the true experimental structure. α-helix (cyan); β-strand (magenta).

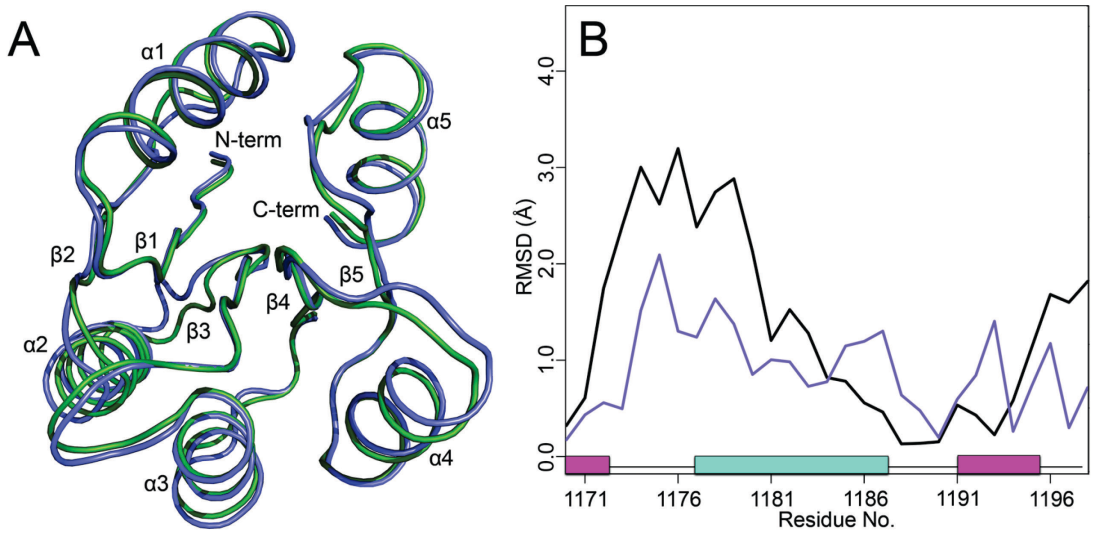

Fig. S15. Global structural alignment of the top representative model to the BeF_3^- bound crystal structure of Sln1-rec and comparisons of the β4-α4-β5 region. (A) Final predicted model (purple). Crystal structure of Sln1-rec with BeF_3^- bound (PDB 2R25:B, green). (B) Per-residue RMSD for apo vs. BeF_3^- crystals (black), and for predicted model vs. BeF_3^- crystal (purple). The black trace shows the differences between the BeF_3^- and apo conformation. The purple trace shows how closely the prediction matches the true experimental structure. α-helix (cyan); β-strand (magenta).

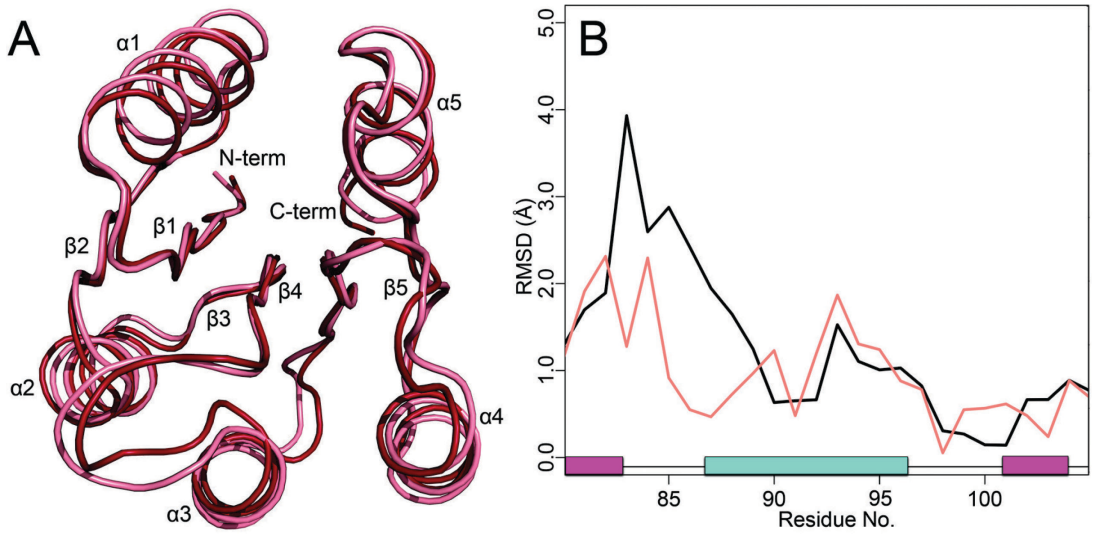

Fig. S16. Global structural alignment of the top representative model to the BeF_3^- bound crystal structure of Spo0F and comparisons of the β4-α4-β5 region. (A) Final predicted model (pink). Crystal structure of Spo0F with BeF_3^- bound (PDB 2FTK:G, red). (B) Per-residue RMSD for apo vs. BeF_3^- crystals (black), and for predicted model vs. BeF_3^- crystal (pink). The black trace shows the differences between the BeF_3^- and apo conformation. The pink trace shows how closely the prediction matches the true experimental structure. α-helix (cyan); β-strand (magenta).

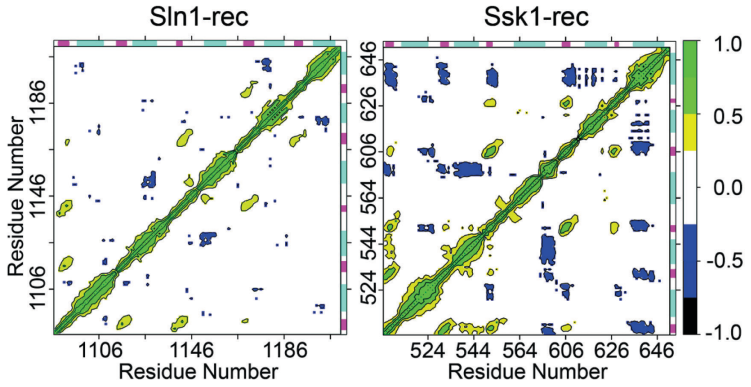

Fig. S17. Dynamical cross-correlation maps for Sln1-rec and Ssk1-rec. Positive correlation (yellow/green) suggests movement in phase, or in the same direction. Negative correlation (blue/black) suggests movement out of phase, or along the opposite direction. α-helix (cyan); β-strand (magenta).

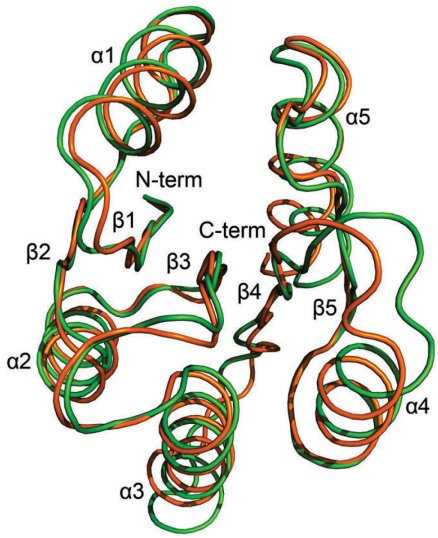

Fig. S18. Global structural alignment of the top predicted model to apo Ssk1-rec. (A) Final predicted model (orange). Apo homology model of Ssk1-rec (green).